SSNV186 – LBB condition and contact rubbing with X-FEM

Summary

The purpose of this test is to validate the taking into account of the contact (by the method continues [bib1]) on the lips of the crack within the framework of method X-FEM [bib2], when the LBB condition [bib3] [bib4] is not respected.

The contact/friction is treated by an algorithm of Lagrangian increased for modelings A with H and by an algorithm penalized for modelings I with K.

This test brings into play a parallelepipedic block in compression. The interface the beam is represented by a level set. The interface is right, not-leaning and crosses the elements completely.

1 Problem of reference

Oscillations of contact pressures can appear in certain cases, in particular for structures where the interface cuts pentahedrons, under a non-uniform loading.

That is due to the non-observance of the LBB condition [bib3] [bib4]. This phenomenon of oscillations is comparable to that met of incompressibility [bib5]. Physically, in the case of the contact, that amount wanting to impose the contact in too many points of the interface (overstrained), making the system hyperstatic. To slacken it, it is necessary to restrict the space of the multipliers of Lagrange, as that is done in [bib6] for the conditions of Dirichlet with X-FEMr. Of such algorithm present P0 segments, which slow down convergence. A good algorithm must minimize the appearance of such segments. The algorithm proposed by Moës [bib6] to reduce the oscillations is adapted to the case 3D (algorithm version 1). This algorithm was the object of an improvement to make it more physical and more effective (algorithm version 2). A comparison of the two versions is carried out.

It should be noted that these parasitic oscillations are not reproducible in the current version of Code_Aster: one of the two algorithms is systematically selected (the 2 is used by default), and even an overload of the code to use some no would bring a null pivot. We illustrate them in this documentation by results resulting from another formulation (formulation with the edges [bib7]), now reabsorbed.

For horizontally cut hexahedrons or quadrangles, there are no P0 segments.

1.1 Geometry

The structure is a right at square base and healthy parallelepiped. Dimensions of the block are: $LX = 5\,m$, $LY = 20\,m$ and $LZ = 20\,m$. It does not comprise any crack [Figure 1.1-1].

The interface is introduced by functions of levels (level sets) directly into the command file using the operator DEFI_FISS_XFEM [U4.82.08]. The interface is present within the structure by the means of its representation by the level sets. The level set normal (LSN) allows to define an interface planes not-leaning which crosses the elements completely, by the following equation:

$$LSN = Z - 17.5$$ **éq 1.1-1**

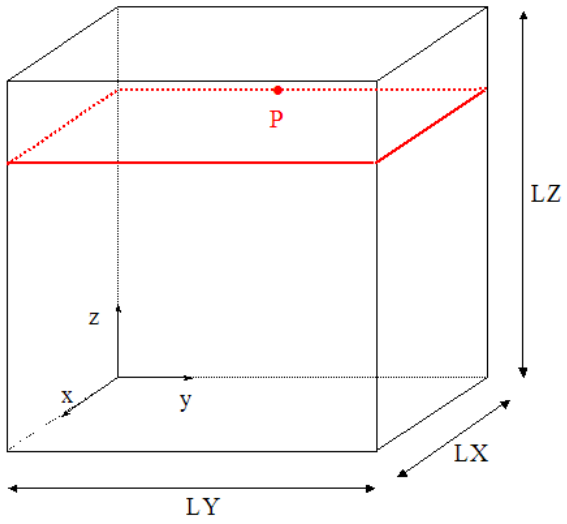

Figure 1.1-1 : Geometry and positioning of the interface

1.2 Properties of material

Young modulus: $E = 100\,GPa$.
Poisson's ratio: $\nu = 0$.

1.3 Boundary conditions and loadings

The lower face is embedded.
The higher face is subjected to a parabolic pressure having for expression:

$$pression = \left(100 - \frac{(Y-10)^2}{2}\right)\frac{E}{10^6}\,Pa$$ **éq 1.3-1**

Displacements along the axes x and y are blocked for the nodes of the upper surface.

1.4 Bibliography

1. Massin P., Ben Dhia H., Zarroug Mr.: Elements of contacts derived from a continuous hybrid formulation, Handbook of reference of *Code_Aster*, [R5.03.52]

2. Massin P., Geniaut S.: Method X-FEM, Handbook of reference of *Code_Aster*, [R7.02.12]

3. Babuška I.: The finite element method with lagrangian multipliers, Numerische Maths 20.179 - 192, 1973

4. Barbosa H., Hugues T.: Finite element method with lagrange multipliers one the boundary. Circumventing the Babuška-Brezzi condition, comp. Meth. Applied Mech Engrg. 85 (1), 109 - 128, 1991

5. Vault D., Bathe K.J.: The Inf-sup test, Computers & Structures 47 (4/5), 537-545, 1993

6. Moës NR., Béchet E., Peaty Mr.: Imposing Dirichlet boundary conditions in the extended finite element method, Int. J. Numer. Meth. Engng, 2006, vol. 67(12), 1641-1699.

7. Géniaut S., Massin P., Moës NR., A stable 3D contact formulation using X-FEM, European Newspaper of Computational Mechanics, Vol.16, n°2, Pages 259-276, 2007.

2 Modeling a: hexahedrons (version 2)

In this modeling, the grid considered comprises only hexahedrons. This modeling is used as reference for the autrbe, because this case does not present P0 segments. Indeed, in the case as of hexahedrons cut by an interface parallel to the faces, the number of contact pressures (one by cut edge) is compatible with the discretization of the field of displacement [bib1] [bib2].

2.1 Characteristics of the grid

The problem is invariant following the axis Ox. In order to limit the computing time, the grid considered here comprises one element along this axis. The structure is then modelled by a regular grid composed of $1\times 20\times 20$ HEXA8 to see [Figure 2.1-1].

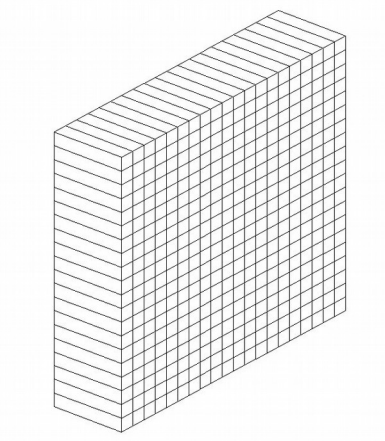

Figure 2.1-1 : Grid of hexahedrons

This grid is composed of linear finite elements. Within the framework of the continuous method [bib1] with X-FEM [bib2], the unknown factors of contact are carried by the nodes tops.

2.2 Features tested

One uses the diagram of integration reduced to 4 points of Gauss per facet of contact.
Friction is taken into account and the contact is active as of the 1era iteration of active constraints.

2.3 Sizes tested and results

One tests the value of the contact pressure at the point P coordinates $(0,10,17.5)$. This value is used as reference for other modelings.

$$\lambda=-9528440\,Pa$$

3 Modeling b: pentahedrons and adherent law (version 2)

In this modeling, one tests the effectiveness of the algorithm version 2 for a grid pentaedric, in the case of an entirely adherent interface. In order to model this one, the cohesive law is used CZM_LIN_MIX.

3.1 Characteristics of the grid

The structure is modelled by a regular grid composed of pentahedrons HEXA6 (see fig.3.1-1).

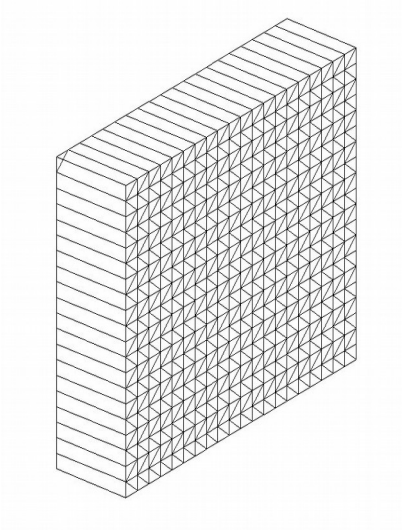

Figure 3.1-1 : Grid of pentahedrons

3.2 Features tested

One validates the use of the algorithm version 2 for an adherent interface.
One validates the implementation of the cohesive law CZM_LIN_MIX for the pentahedral elements.
One uses the diagram of integration reduced to 4 points of Gauss per facet of contact.
The cohesive law CZM_LIN_MIX is used with a critical stress σ_c much higher than the pressure applied (defined by the equation 1.3-1): $\sigma_c = 50\times10^6\ Pa$. Thus, the constraint criticizes will never be exceeded during calculation: the interface thus remains adherent.

3.3 Sizes tested and results

One tests the value of the contact pressure at the point P coordinates $(0,10,17.5)$, the value of reference being that of modeling A .

Identification	Reference	% difference
Not P	-9528440	1.0

4 Modeling C: triangles and adherent law (version 2)

In this modeling, one tests the effectiveness of the algorithm version 2 for a triangular grid, in the case of an entirely adherent interface. In order to model this one, one uses cohesive law CZM_LIN_MIX.

4.1 Characteristics of the grid

The structure is modelled by a regular grid composed of pentahedrons TRIA3 (see fig.4.1-1).

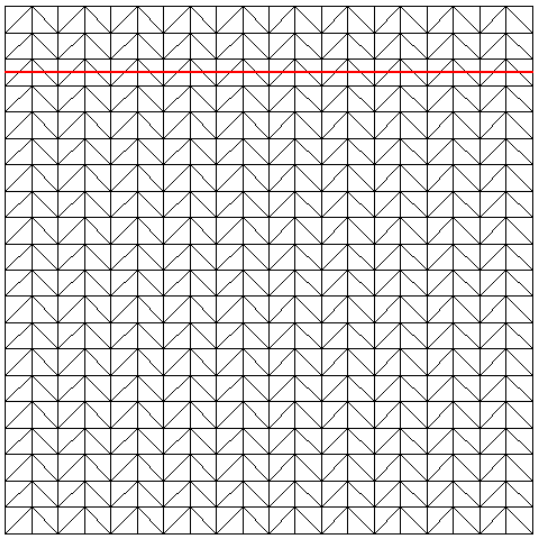

Figure 4.1-1 : Grid of triangles

4.2 Features tested

One validates the use of the algorithm version 2 for an adherent interface.
One validates the implementation of the cohesive law CZM_LIN_MIX for the elements triangles.
The cohesive law CZM_LIN_MIX is used with a critical stress σ_c much higher than the pressure applied (defined by the equation 1.3-1): $\sigma_c = 50\times10^6\ Pa$. Thus, the constraint criticizes will never be exceeded during calculation: the interface thus remains adherent.

4.3 Sizes tested and results

One tests the value of the contact pressure at the point P coordinates $(0,10,17.5)$, the value of reference being that of modeling A.

Identification	Reference	% difference
Not P	-9528440	0.7

5 Modeling D: pentahedrons and friction

5.1 Characteristics of the grid

The grid is identical to that of modeling B.

5.2 Features tested

One uses the diagram of integration reduced to 4 points of Gauss per facet of contact.
Friction is taken into account and the contact is active as of the 1era iteration of active constraints.
The algorithm aiming at restricting the space of the multipliers of Lagrange is the n°2.

5.3 Sizes tested and results

One tests the value of the contact pressure at the point P coordinates $(0,10,17.5)$.

Identification	Reference	% difference
Not P	-9528440	0.10

5.4 Comments

This modeling shows that the algorithm version 2 makes it possible to reduce the oscillations efficiently. It is observed that the algorithm version 2 tends to introduce approximations $P1$ by pieces of contact pressures on the interface, which makes it more precise than the version1 (see also it [Figure 7.2-1] and it [Figure 7.2-2]).

6 Modeling E: tetrahedrons (algorithm version 1)

This test brings into play a free grid made up of tetrahedrons. In order to reduce the number of elements and thus the computing time, the length of the structure along the axis Ox is $LX = 1\ m$.

6.1 Characteristics of the grid

The grid considered is a free grid carried out with GMSH. It consists of 3629 TETRA4. [Figure 6.1-1] the grid in the plan represents Oyz . The interface is traced there only at ends of visualization.

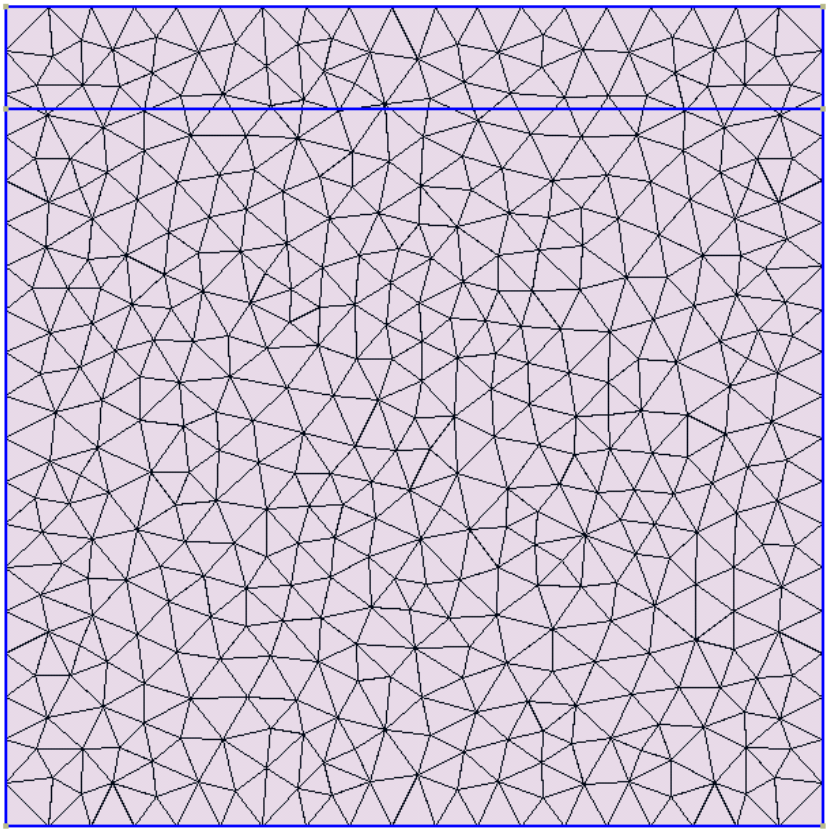

Figure 6.1-1 : Free grid

6.2 Boundary conditions and loadings

The lower face is embedded.
The higher face is subjected to a uniform pressure:

$$pression = 100 \frac{E}{10^6} Pa$$ **éq 6.2-1**

Displacements along the axes x and y are blocked for the nodes of the upper surface.

6.3 Features tested

One uses the diagram of integration reduced to 4 points of Gauss per facet of contact.
The contact is active as of the 1era iteration of active constraints but friction is not taken into account
The algorithm aiming at restricting the space of the multipliers of Lagrange is the n°1.

6.4 Sizes tested and results

One tests the value of contact pressures for all the points of the interface. The analytical solution is quite simply:

$$\lambda = \sigma_{zz} = -pression \qquad \textbf{éq 6.4-1}$$

Identification	Reference	% difference
MAX (LAGS_C)	-10E7	0.01 %
MIN (LAGS_C)	-10E7	0.01 %

To test all the points of contact in only once, one tests the minimum and the maximum of column.

6.5 Comments

This test makes it possible to validate the robustness of the algorithm of restriction of the space of the multipliers of Lagrange of pressure, in a free case of grid in 3D. Even on a structure subjected to constant pressure, the algorithm is essential bus of the oscillations of contact pressures can appear (it is the case here if the algorithm is not activated).

7 Summaries of the results 3D

7.1 Summary

Within the framework of method X-FEM, one showed that, without particular treatment, a structure with a grid with pentahedrons subjected to a non-uniform loading can have strong oscillations of contact pressures, like the second curve shows it of [Figure 7.2-1]), realized with a different formulation [bib7], now reabsorbed in Code_Aster, for which the absence of algorithm of restriction did not actuate a null pivot. Leven structure with a grid has with hexahedrons subjected to the same loading does not have such oscillations (modeling A being used as reference).

One proposed two algorithms allowing to reduce these oscillations significantly. The first (third curve of [Figure 7.2-1]) seems less precise than the second (modeling D).

Moreover even under uniform loading, of the oscillations can appear and it is essential to use an algorithm of reduction of the space of the multipliers of Lagrange of pressure (modeling E).

7.2 Curves of comparison

[Figure 7.2-1] gathers the curves of contact pressures along the axis Oy , respectively for the hexahedral grid (modeling A), a grid pentaedric without algorithm of treatment of the LBB, a grid pentaedric with algorithm 1 and finally a grid pentaedric with algorithm 2 (modeling D). It is noticed that the oscillations for the second case are so strong that in certain points the value of the contact pressure becomes positive, which would like to say that there is separation of the interface. The two algorithms allow a visible reduction of the oscillations, and one finds the curve of reference obtained with the grid of hexahedrons.

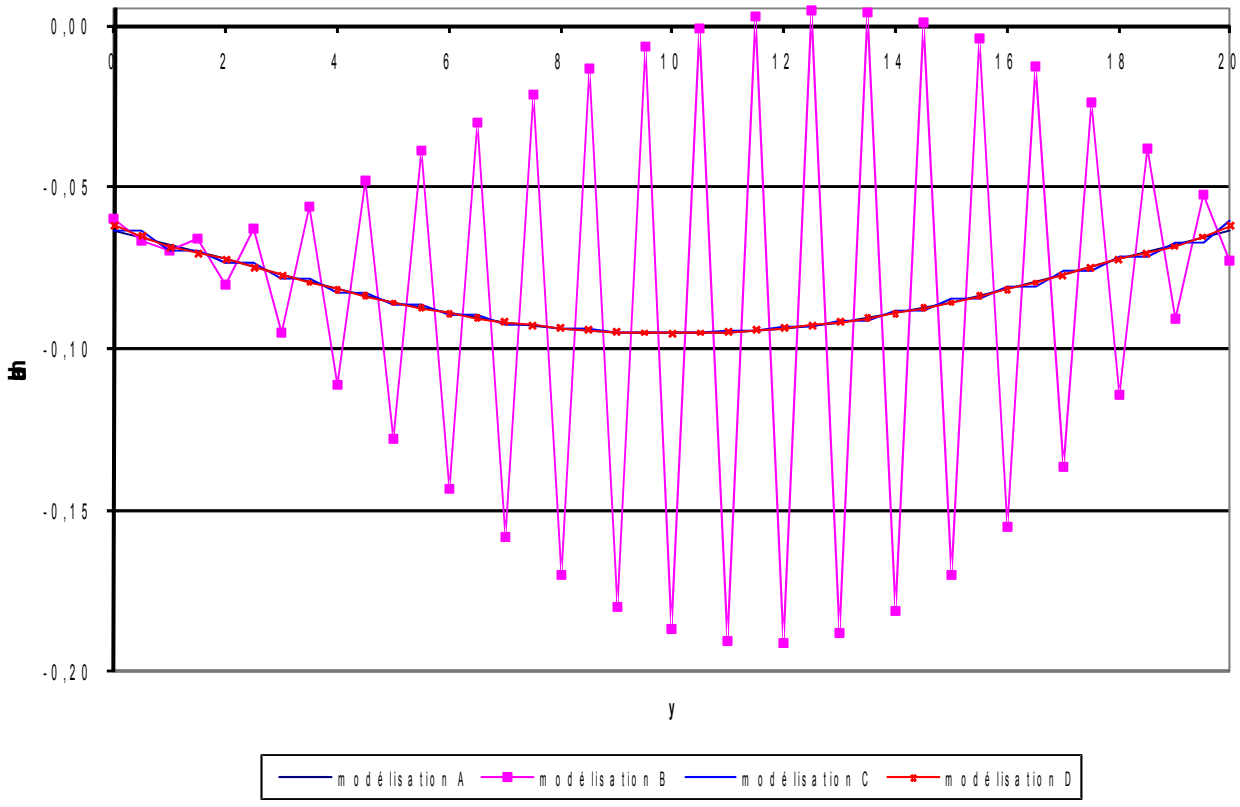

Figure 7.2-1 : Comparison of contact pressures following modelings (pressures expressed in GPa)

[Figure 7.2-2] compares in details the effects of the two algorithms. It is noticed that the first often implies constant contact pressures per pieces, whereas the second tends to linearize the pressures. It is obvious that such differences are reduced by refining the grid.

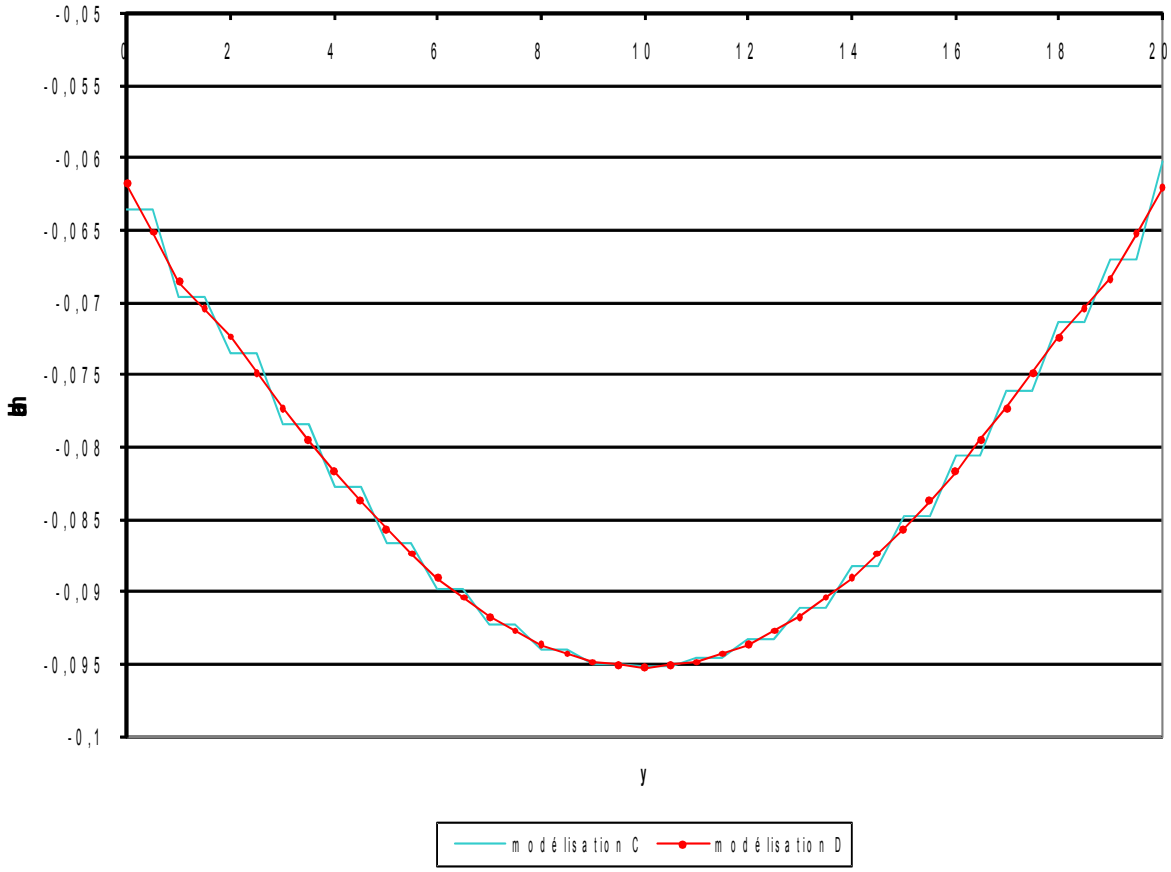

Figure 7.2-2 : Comparison of the 2 algorithms (pressures expressed in GPa)

8 Modeling F: quadrangles 2D

This modeling is the equivalent in 2D of modeling A (reference). This case does not have oscillations of contact pressures. Just like in modeling A, the quadrangles are crossed by an interface parallel to the edges. There are then no P0 segments.

8.1 Characteristics of the grid

The structure is then modelled by a regular grid composed of 20×20 QUAD4 (See [Figure 8.1-1]).

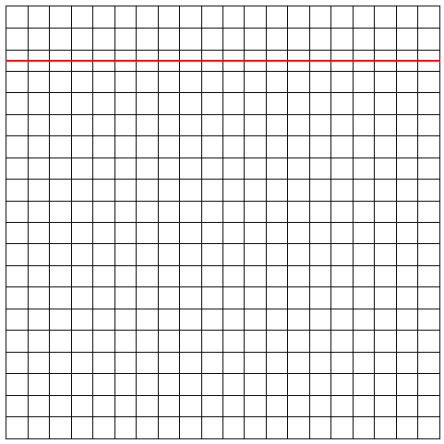

Figure 8.1-1 : Grid of quadrangles

8.2 Features tested

Friction is taken into account and the contact is active as of the 1era iteration of active constraints. The algorithm aiming at restricting the space of the multipliers of Lagrange is number 2.

8.3 Sizes tested and results

One tests the value of the contact pressure at the point P coordinates $(10,17.5)$.

Identification	Reference	% difference
Not P	-9528440	$2.41\,10^{-4}$

8.4 Comments

This case test makes it possible to find the values of reference of contact pressures calculated in modeling A, and to check that in the case of quadrangles parallel to cut their faces, these contact pressures do not present P0 segments (see [Figure 11.2-1]).

9 Modeling G: triangles (algorithm version 1)

9.1 Characteristics of the grid

The structure is modelled by a regular grid composed of triangles. The test is the equivalent in 2D of modeling B (See [Figure 9.1-1]).

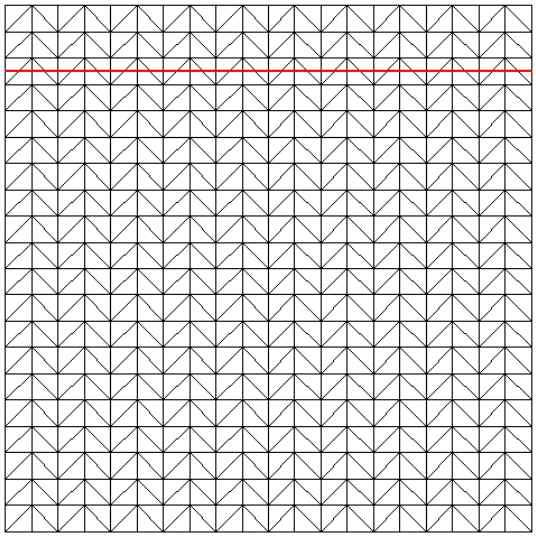

Figure 9.1-1 : Grid of triangles

9.2 Features tested

Friction is taken into account and the contact is active as of the 1era iteration of active constraints. The algorithm aiming at restricting the space of the multipliers of Lagrange is the n°1.

9.3 Sizes tested and results

One tests the value of the contact pressure at the point P coordinates $(10,17.5)$.

Identification	Reference	% difference
Not P	-9528440	0,655

9.4 Comments

This modeling shows that the algorithm set up makes it possible to reduce the oscillations effectively. (see [Figure 11.2-1]).

10 Modeling H: triangles (algorithme version 2)

10.1 Characteristics of the grid

The grid is identical to that of modeling G.

10.2 Features tested

Friction is taken into account and the contact is active as of the 1era iteration of active constraints. The algorithm aiming at restricting the space of the multipliers of Lagrange is the n°2.

10.3 Sizes tested and results

One tests the value of the contact pressure at the point P coordinates $(10,17.5)$.

Identification	Reference	% difference
Not P	-9528440	0,655

10.4 Comments

This modeling shows that in 2D, the algorithm version 2 has a behavior very close to that of version 1. Indeed, put except for the first contact pressures measured on the left of the grid, the actual values are identical, and the curves obtained with the two algorithms are recovered almost completely. (see [Figure 11.2-1]).

11 Summaries of the 2D results

11.1 Summary

It, initially, was checked that the behavior of the structure of reference (modeling A) could be found in 2D (modeling F). After having observed the phenomenon of oscillations in 2D, one tested on cases in 2D the two algorithms which make it possible to reduce these oscillations in 3D.

The two algorithms tested in modelings G and H give, in 2 dimensions, of the very close results, and make it possible consequently to reduce the oscillations introduced by the grid.

11.2 Curves of comparison

[Figure 11.2-1] represents the curves of contact pressures along axis OX for 3 modelings in 2D presented. It is noticed that the curves representative of the two algorithms are recovered almost completely. The two algorithms are thus about as efficient one as the other in 2D. It make it possible nevertheless to reduce the oscillations effectively.

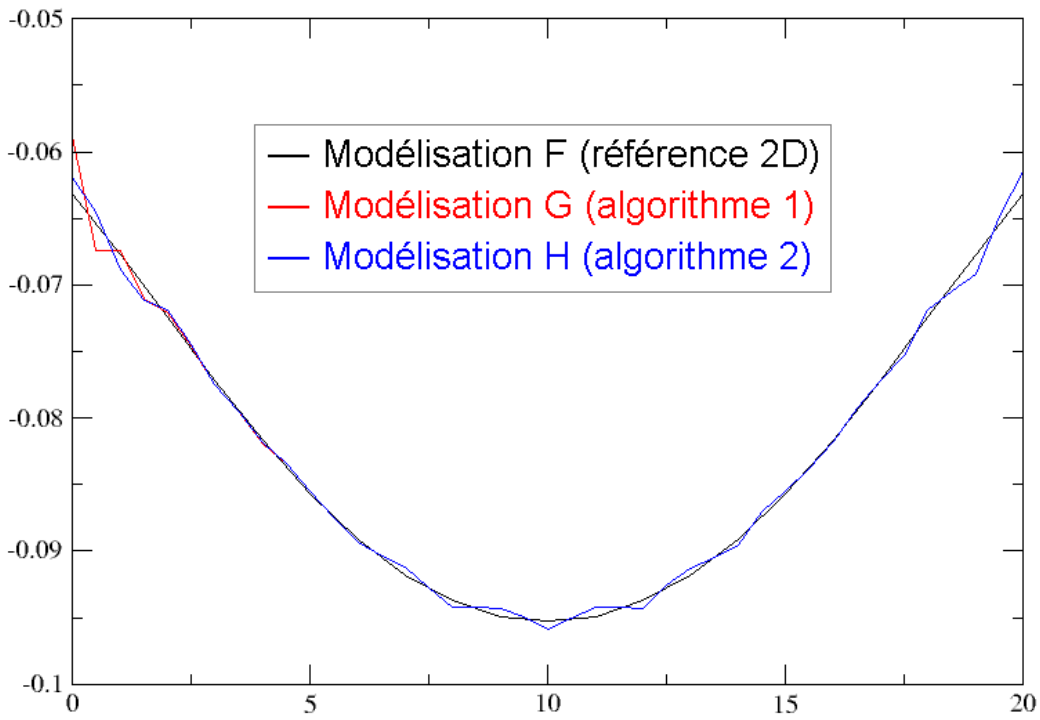

Figure 11.2-1 : Comparison of contact pressures following modelings 2D (pressure expressed in GPa).

It is it should be noted that a refinement of grid increases obviously the precision of the got results.

12 Modeling I: pentahedrons (algorithm version 2), penalized method

12.1 Characteristics of the grid

The grid is identical to that of modeling B.

12.2 Features tested

One uses the diagram of integration reduced to 4 points of Gauss per facet of contact.
Friction is taken into account and the contact is active as of the 1era iteration of active constraints.
The algorithm aiming at restricting the space of the multipliers of Lagrange is the n°2.

12.3 Sizes tested and results

One tests the value of the contact pressure at the point P coordinates $(0,10,17.5)$.

Identification	Reference	% difference
Not P	$\lambda=-9528440\,Pa$	$4.4\,10^{-3}$

12.4 Comments

One finds results comparable to those of modeling B where the algorithm of contact/friction was the Lagrangian one increased, and this, on all the surface of contact (see [Figure 26.2.1]).

13 MODelisation J: tetrahedrons (algorithm version 1), penalized method

This test brings into play a free grid made up of tetrahedrons. In order to reduce the number of elements and thus the tempS of calculation, the length of the structure along the axis Ox is $LX = 1\ m$.

13.1 Characteristics of the grid

The grid is identical to that of modeling E.

13.2 Boundary conditions and loadings

The lower face is embedded.
The higher face is subjected to a uniform pressure:

$$pression = 100 \frac{E}{10^6} Pa \qquad \text{éq 13.2-1}$$

Displacements along the axes x and y are blocked for the nodes of the upper surface.

13.3 Features tested

One uses the diagram of integration reduced to 4 points of Gauss per facet of contact.
The contact is active as of the first iteration of active constraints.
The algorithm aiming at restricting the space of the multipliers of Lagrange is the n°1.
One tests here the method penalized to treat the contact/friction.

13.4 Sizes tested and results

One tests the value of contact pressures for all the points of the interface. The analytical solution is quite simply:

$$\lambda = \sigma_{zz} = - pression \qquad \text{éq 13.4-1}$$

Identification	Reference	% difference
MAX (LAGS_C)	-10E7	10^{-4}
MIN (LAGS_C)	-10E7	10^{-4}

To test all the points of contact in only once, one tests the MINIMUM and the maximum of column.

13.5 Comments

One finds results comparable to those of modeling E where the algorithm of contact/friction was the Lagrangian one increased.

14 Modelisation K: triangles (algorithm version 1), penalized method

14.1 Characteristics of the grid

The grid is identical to that of modeling G.

14.2 Features tested

Friction is taken into account and the contact is active as of the first iteration of active constraints.
The algorithm aiming at restricting the space of the multipliers of Lagrange is the n°1.
One tests here the method penalized to treat the contact/friction.

14.3 Sizes tested and results

One tests the value of the contact pressure at the point P coordinates (10, 17.5).

Identification	Reference	% difference
Not P	-9528440	0.30

14.4 Comments

One finds results comparable to those of modeling G where the algorithm of contact/friction was the Lagrangian one increased, and this, on all the surface of contact (see [Figure 26.2.2]).

15 Summaries of the results of penalized method

15.1 Summary

It was shown that the penalized method made it possible to satisfy the LBB condition as well as the method of Lagrangian increased.

15.2 Curves of comparison

Figures 26.2.1 and 26.2.2 show the profile of contact pressure along the interface when one uses the penalized method and the method of Lagrangian increased. The results of modelings A and F are given as reference. It is noted that it has there very little difference between the results of the two methods.

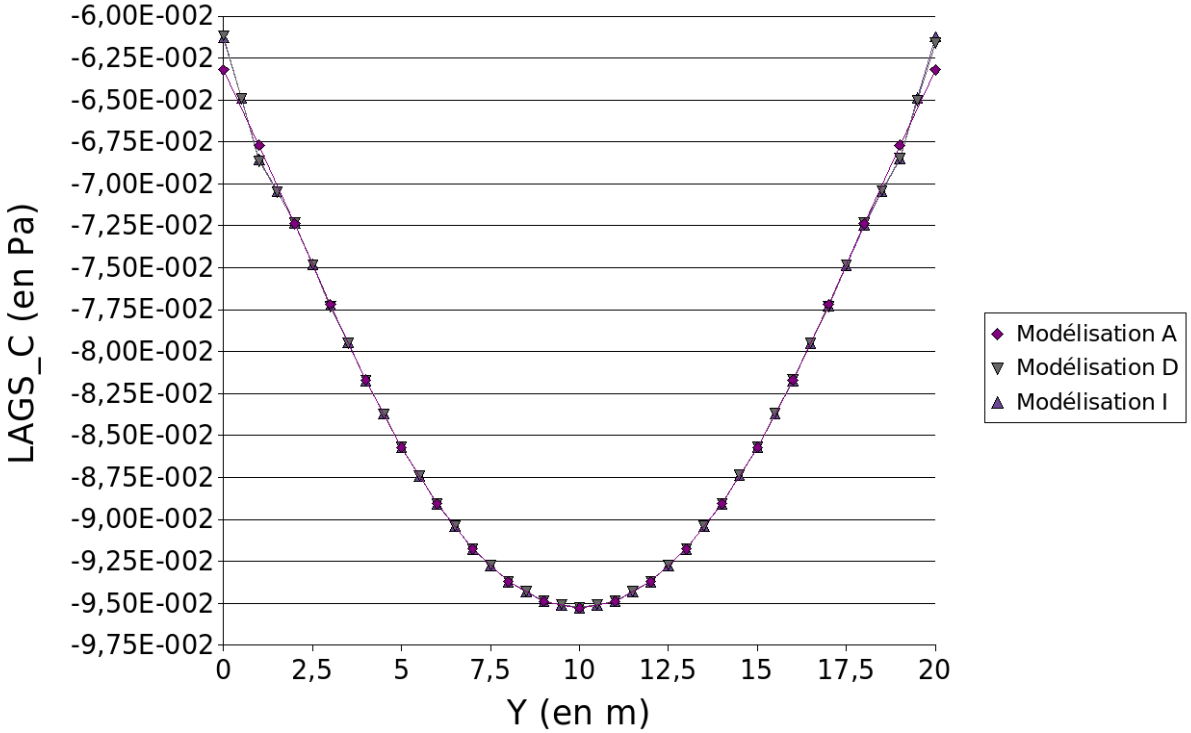

Figure 15.2-1: Comparison of the method of Lagrangian increased and the method penalized in 3D.

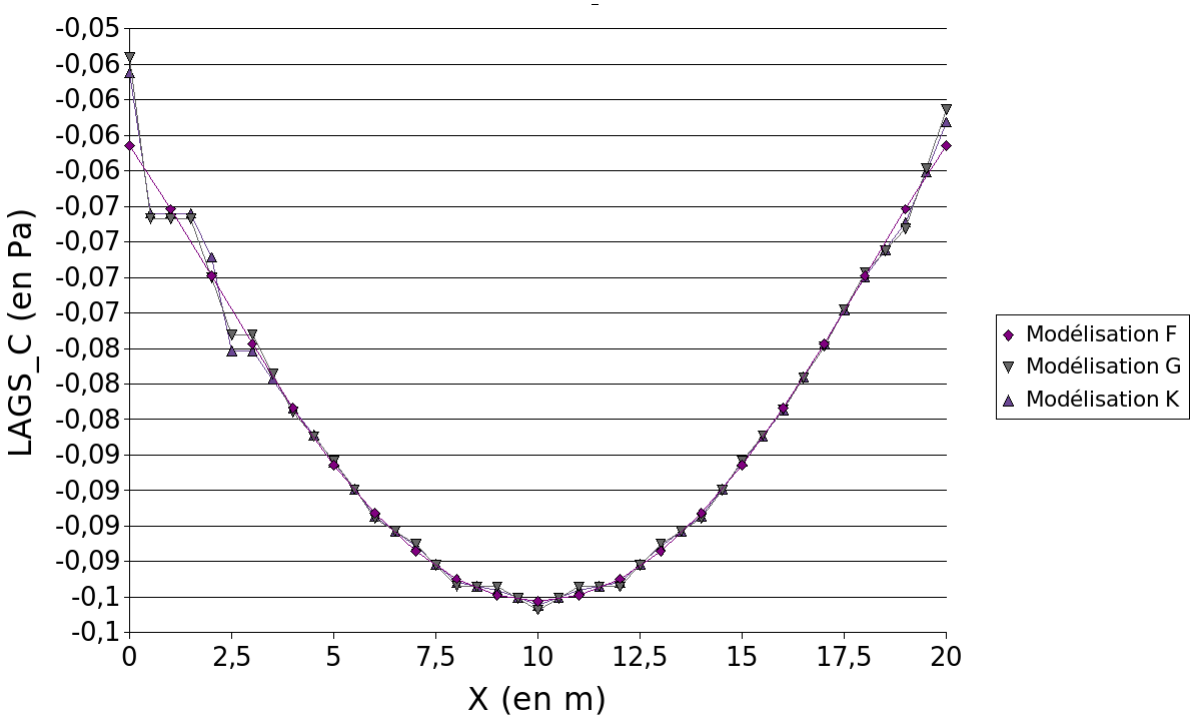

Figure 15.2-2: Comparison of the method of Lagrangian increased and the method penalized in 2D.

16 Modeling L: pyramids (algorithm version 2)

16.1 Characteristics of the grid

The grid in linear elements consists of hexahedrons, tetrahedrons and pyramids. The crack illustrated in blue on Figure 16.1-1cross part of the pyramids and tetrahedrons in their medium.

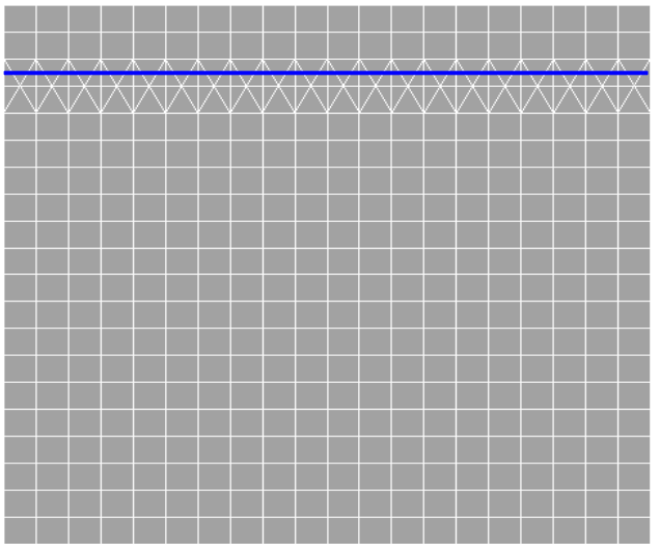

Figure 16.1-1: Grid of hexahedrons, tetrahedrons and pyramids

16.2 Features tested

Friction is taken into account and the contact is active as of the first iteration of active constraints. Unknown contact pressures are put at Nœuds of the elements. The algorithm aiming at restricting the space of the multipliers of Lagrange is the n°2. The elements pyramid here are tested.

16.3 Sizes tested and results

One tests the value of the contact pressure at the point $P1$ and $P2$ respective coordinates $(0,10,17.)$ and $(0,10,18.)$. These nodes are the tops of the edge passing by the point P $(0,10,17.5)$.

Identification	Reference	% difference
Points $P1$ and $P2$	-9528440	0.0351

16.4 Curves of comparison

[Figure 16.4-1] represents the curves of contact pressures along the axis Oy with $x=0$ for modelings A and L. One took the values in $z=17$ for modeling M since there is no point in $z=17.5$ as for modeling A. One notices all the same that the curve of modeling L follows well the curve of reference obtained with the grid of hexahedrons.

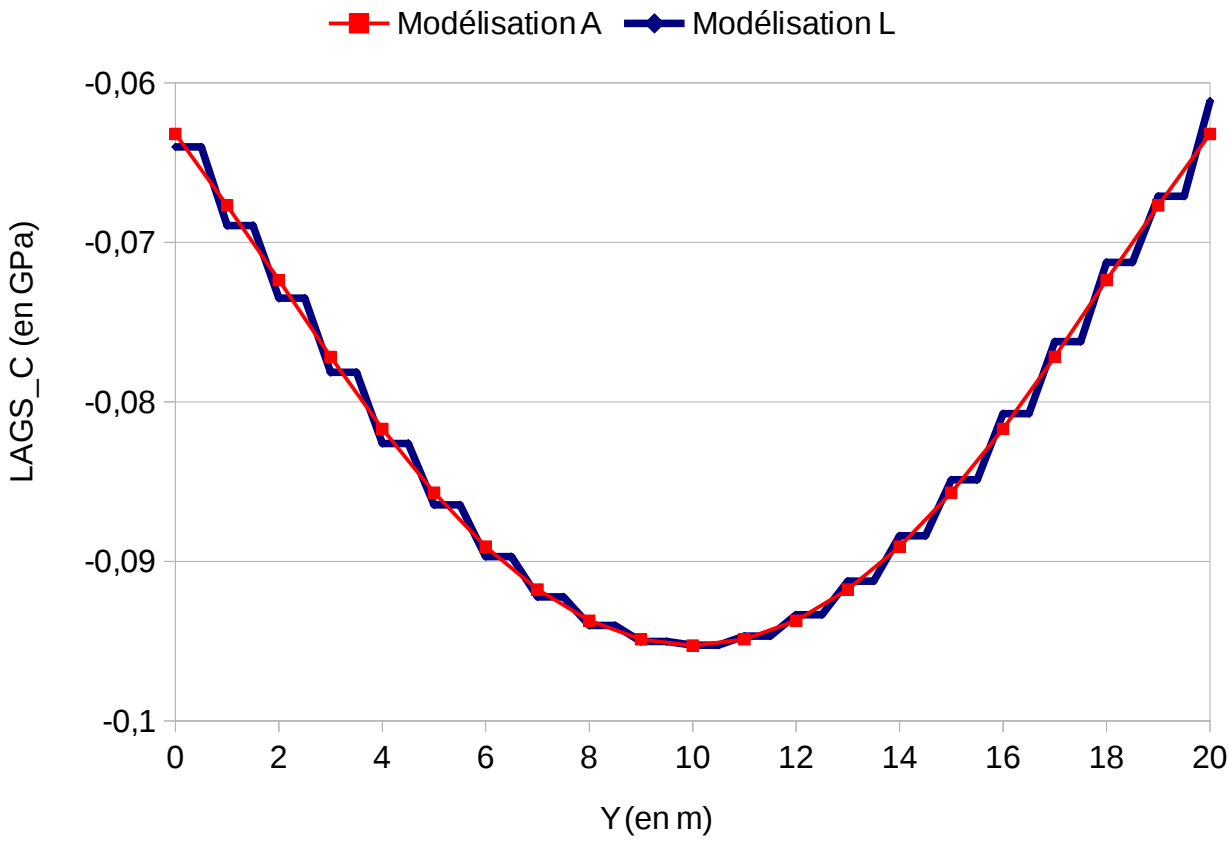

Figure 16.4-1: Comparison of contact pressures following modelings

16.5 Comments

One finds results comparable to those of modeling A where the whole of the grid of the structure contains hexahedrons. The introduction of the pyramids into the grid to the level surface of contact deteriorate little the results of contact pressures.

17 Modeling M: pyramids (algorithm version 2)

17.1 Characteristics of the grid

The grid of modeling M takes again the grid of modeling L while passing it into quadratic. It consists of hexahedrons, tetrahedrons and pyramids. The crack illustrated in blue on Figure 16.1-1 cross part of the pyramids and tetrahedrons in their medium.

17.2 Features tested

Friction is taken into account and the contact is active as of the first iteration of active constraints. Unknown contact pressures are put at Nœuds of the elements. The algorithm aiming at restricting the space of the multipliers of Lagrange is the n°2. One tests here the elements pyramid into quadratic (PYRA13).

17.3 Sizes tested and results

One tests the value of the contact pressure at the point P coordinates (10, 17.5).

Identification	Reference	% difference
Not P	-9528440	0.025

17.4 Curves of contact pressure

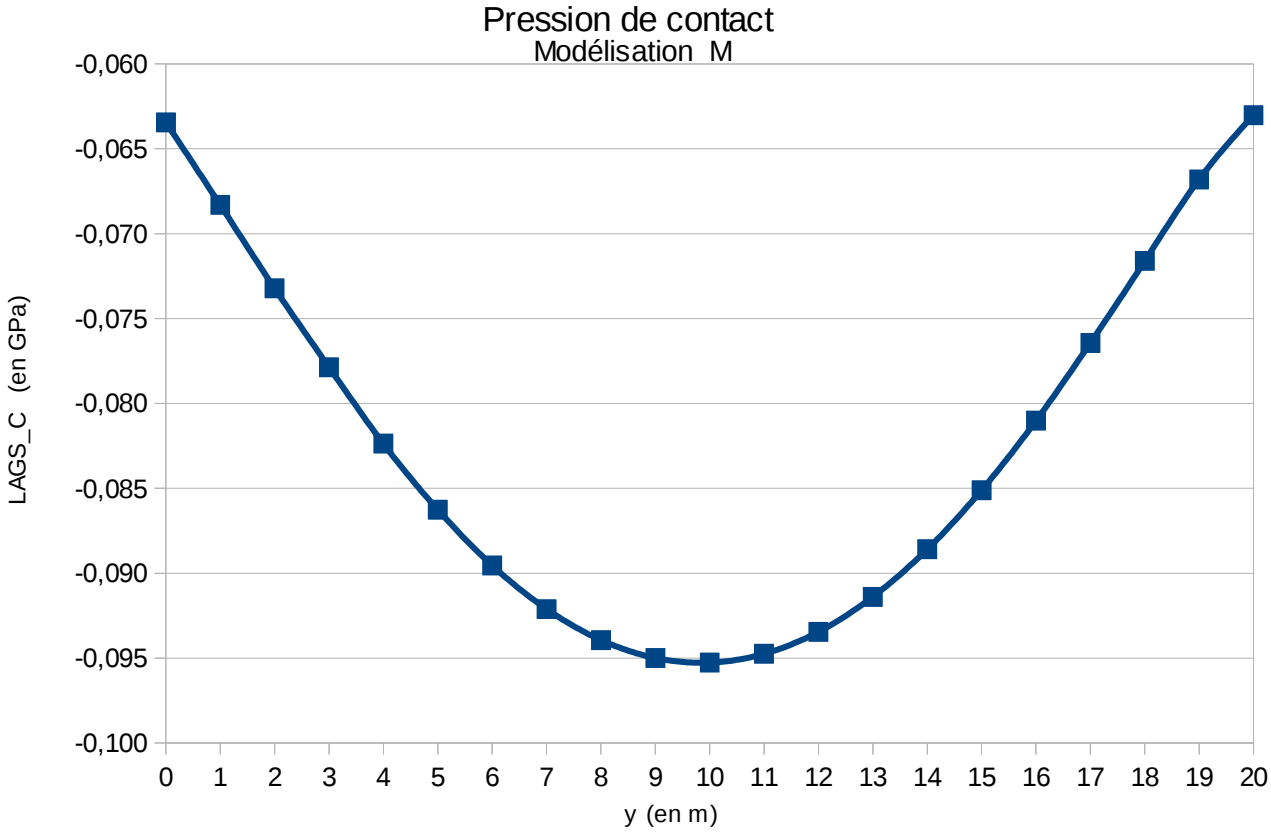

Figure 17.4-1: Evolution of the contact pressure following axis OY.

17.5 Comments

The results of quadratic modeling are comparable to those of preceding modelings linear. This modeling makes it possible to validate the quadratic use of pyramids with method X-FEM and of the contact.